ARTICLE

Zn Cluster Drifting Effect for the Formation of ZnO 3D Nanoarchitecture

Jian Shi,[†] Scott Grutzik,[‡] and Xudong Wang[†,*]

[†]Department of Materials Science and Engineering and [‡]Department of Engineering Physics, University of Wisconsin at Madison, Madison, Wisconsin 53706-1595

ABSTRACT Metal catalysts are widely used for nanowire (NW) growth and are one of the essential parameters that dictate the crystal growth phenomena, thus controlling the NW's morphology. Although extensive research has been conducted on catalyst effects, the catalyst drifting effect is generally underestimated for controlling the morphology of nanostructures grown at a relatively high temperature. In this paper, we report a discovery of Zn cluster drifting phenomenon during ZnO vapor deposition. Because of the deposition of ZnO along the drifting path, the dynamic process of cluster drifting could be visualized after the growth. This phenomenon provides a sound explanation of the formation of randomly orientated ZnO nanowall networks. The cluster drifting direction could be intentionally directed by designing the surface inclination, through which a partially parallel aligned ZnO vertical nanofin array was created. This 3D nanoarchitecture would possibly provide a novel configuration for designing high performance integrated nanodevices. The drifting of Zn clusters could be a general phenomenon for most metal catalysts and would provide a new insight into nanofabrication and nanodevice development.

KEYWORDS: zinc oxide · nanofin array · finFET · nanowall · nanowire · catalyst drifting

Starting with the discovery of carbon nanotubes in the early 1990s,[1] followed by extensive development of semiconducting nanowires (NWs),[2−4] one-dimensional (1D) nanostructures have quickly been considered a key technology for the next generation of high performance nanodevices in the areas of electronics,[5,6] photonics,[7,8] optoelectronics,[9−11] mechanics,[12−14] biosensors/detectors,[15−17] and so on. Among them, zinc oxide (ZnO) is known as an important technology material due to its interesting semiconducting and piezoelectric properties. 1D ZnO nanostructures, including NWs[18] and nanobelts,[19] have been demonstrated as a good candidate for solid state laser diodes[20] and light emitting diodes (LEDs)[21] in the near UV range due to its direct 3.37 eV bandgap with a high exiton binding energy (60 meV). ZnO NWs also exhibit great promise in the application of field effect transistors (FETs), spintronics, transducers, and sensors.[22,23] The coupling of semiconductor and piezoelectric properties in ZnO NWs recently provided opportunities in micro or nanoscale mechanical energy harvesting.[24,25]

To sustain the rapid development of NW-based technology, one essential issue is to provide reliable NW building blocks with controlled composition, dimension, orientation, and position over a large quantity. Recently, vertically aligned growth of NWs has been shown as an effective way to organize NWs during growth for immediate nanodevice fabrication and integration.[20,26] In such a process, a metallic catalyst is typically used for determining the NW position, directing the anisotropic crystal growth, and confining the size through a vapor−liquid−solid (VLS) process.[27,28] Aligned NWs could also be synthesized without catalysts. In this case, it is generally believed that the metal clusters, such as Zn from ZnO, would act as the nucleation sites.[29] Research has shown that the catalysts, either predeposited foreign metal or self-generated clusters from the source, could exhibit diffusion phenomenon along or within the NWs during the growth at high temperature.[30,31] However, few insights have been put forth about the initial stage before the growth of NWs. In general, catalysts are considered staying at where they were deposited, thus determining the location and distribution of NWs. This is true for most cases; but under certain circumstances, catalysts might be able to move prior to the formation of NWs, particularly when the deposition temperature is high. This effect would be of great importance in practical applications of the VLS process as well as for understanding certain growth phenomena, such as horizontally aligned growth of NWs,[32,33] and the

*Address correspondence to xudong@engr.wisc.edu.

Received for review April 20, 2009 and accepted May 12, 2009.

Published online May 20, 2009.
10.1021/nn900388z CCC: $40.75

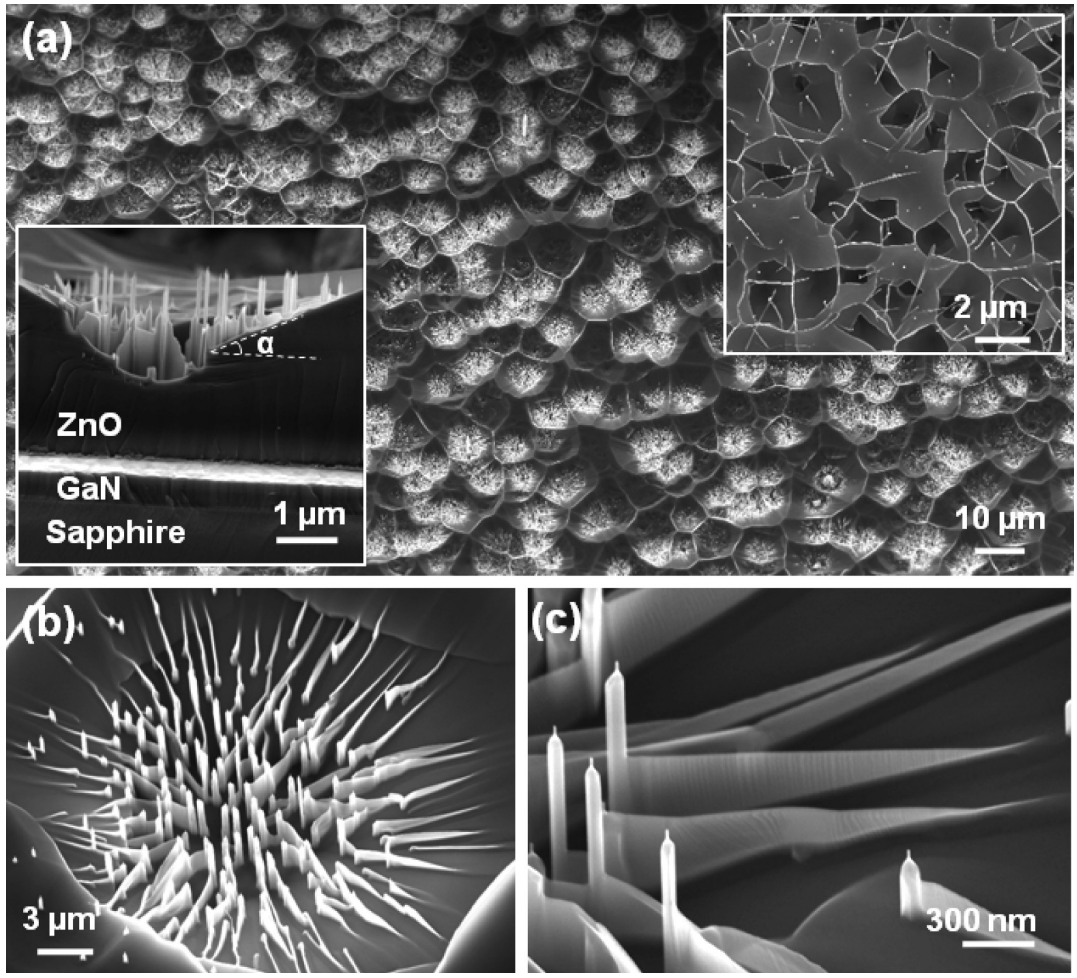

Figure 1. SEM observation of the Zn cluster drifting phenomenon. (a) A low magnification SEM image of the drifting traces located inside the surface concaves of a ZnO epitaxial layer. Inset top-right shows the surface concave structure without the drifting traces. Inset bottom-left shows a cross-section image of the hierarchical structure, which reveals that each trace was formed by a "fin"-like structure terminated at one vertically grown NW. (b) A 30° side-view SEM image showing the distribution of the NW-nanofin structures in one concave surface. (c) A higher magnification 30° side-view SEM image showing the detailed structure of the NW-nanofin structure, where a series of steps can be clearly observed on the nanofin surface indicating curving of the nanofin along the inclined bottom surface.

formation of side branches or bottom networks under vertically aligned NW arrays.[34,35] Nevertheless, due to the vigorous reaction condition, it is very difficult to observe such a phenomenon and perform in-depth investigation.

In this paper, we report a discovery of Zn cluster drifting phenomenon during ZnO vapor deposition. At high Zn vapor concentration, ZnO could be deposited along the drifting path, so that the dynamic process of cluster drifting could be visualized after the growth. This phenomenon provides a sound explanation of the formation mechanism of nanowall network structures. By controlling the drifting direction, a parallel aligned vertical ZnO nanofin array was synthesized, which could be a novel 3D nanoarchitecture for nanodevice assembly and integration.

RESULTS AND DISCUSSION

Observation of Zn Cluster Drifting Phenomenon. In our experiments, the ZnO nanostructures were deposited on GaN epi-layer covered sapphire substrate without using any catalysts. During a vapor deposition process that has been widely used for growing ZnO NWs,[36] when the vapor concentration was significantly increased by reducing the volume of the growth chamber (see details in the experimental section), a two-dimensional film growth condition could be reached and a ZnO epitaxial layer was formed on the (0001) GaN surface. The ZnO layer exhibited a rough surface composed of packed concaves, possibly due to the competition between surface energy and strain energy.[37] These concaves were several micrometers wide and ~2−3 μm deep. NWs could be grown during the furnace cooling process, when the production of Zn vapor was reduced by lowering the temperature, thus bringing the vapor concentration to a lower level that was favorable for 1D NW growth. The scanning electron microscope (SEM) image in Figure 1a shows the secondary NW growth around the centers of most surface concaves on the ZnO layer. The surface concaves are shown

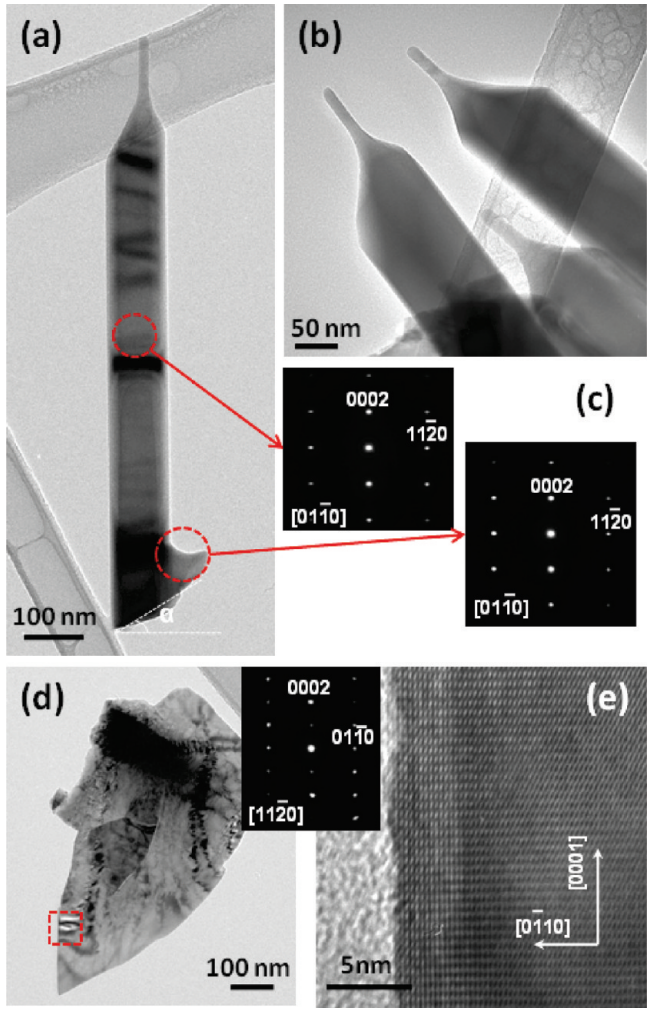

Figure 2. TEM analysis of the ZnO NWs and nanofins: (a) ZnO NW with a small broken nanofin attached at its root; (b) sharp and clean tips of the ZnO NWs showing no foreign catalyst was involved during the growth; (c) selective-area electron diffraction (SEAD) patterns taken on the body and root areas of the NW shown in panel a; (d) broken piece of a nanofin structure, inset is the SEAD pattern showing its single crystalline structure; (e) high resolution TEM image taken in the highlighted area in panel d showing a dislocation free crystal lattice on the flat area on the nanofin.

in the top-right inset of Figure 1a, which was formed by quickly removing the reactive gases from the growth chamber before the cooling process began, so that the substantial NW growth was effectively eliminated. The cross sectional SEM image clearly shows the hierarchical structure (bottom-left inset of Figure 1a). The thickness of the ZnO layer was ~4 to 5 μm at the summit of the concaves and ~2 to 3 μm at the bottom. The slope of the concave surfaces was about 25° to the horizontal plane. Most of the NWs were located around the bottom region of those concaves, and interestingly, most of them carried a long "tail" originating from the top of the concaves.

A side-view SEM image in Figure 1b shows the tails were actually vertical thin films, like a "fin" structure. All the nanofins originated around the edges of the concaves and pointed down along the inclined concave surfaces toward the NWs standing around the bottom. The orientations of the nanofins possibly indicated the drifting trace of the Zn cluster before the formation of NWs since no other catalyst was applied for the growth. The detailed structure of the nanofins is shown in Figure 1c. A typical nanofin was formed by a several-micrometer-long ZnO thin film with a thickness of only tens of nanometers. One end of the nanofin merged with the NW's side wall, while the other end was half "buried" into the concave surface. A very sharp tip was also observed on each ZnO NW, which resulted from the decreasing of reactive vapor concentration during cooling process.

The crystallography of the ZnO NWs and the nanofins was further investigated by transmission electron microscopy (TEM). Figure 2a shows a typical ZnO NW with a broken nanofin attached on its root. The angle between root plane of the nanofin and the horizontal direction was measured to be 27°, which closely matches the slope angle of the concave surfaces, indicating this NW was removed from the concave surfaces. The sharp tip of the NW can be clearly seen from the TEM image. The tip is about 10 nm wide and 100 nm long. At the very front of the small tip, no trace of foreign catalysts could be identified. More tip structures are shown in Figure 2b, all of which exhibited a clean, smooth, fine tip indicating all the NWs were formed by self-catalyzing from zinc clusters. This sharp tip structure is one typical NW morphology when no foreign catalysts are presented during the vapor deposition. Yang *et al*. have already performed a comprehensive microscopy study on the tip's crystal structure and interpreted the formation mechanisms,[38] whereas our intention here is to reveal the catalyst behavior before it initiates the NW growth. Selected-area electron diffraction (SAED) patterns shown in Figure 2c were taken at the body of the ZnO NW and around the residue nanofin region, respectively. Identical SAED patterns were received indicating that the NW and the attached nanofin were one piece of single crystal. As expected, the NWs were grown along the [0001] direction.

One broken piece of a nanofin was collected and shown in Figure 2d. The dark contrast lines were attributed to the bending of the fin. Such bending can be commonly observed on most nanofins as shown in Figure 1. Figure 1c also reveals that curving of the nanofin was composed by stepped side surfaces, which released the bending induced strain energy. Despite the bending, the nanofin exhibits a single crystalline crystal structure as shown by the SAED pattern (inset of Figure 2d). High resolution TEM image taken along the edge of the nanofin (indicated by the dashed square box in Figure 2d) revealed a dislocation-free structure on the flat area (Figure 2e). Therefore, from the TEM analysis, it can be confirmed that the ZnO NW and its attached nanofin are one piece of single crystal.

Surface Effects on Zn Cluster Drifting. Figure 3a shows a top view of several surface concaves, where all the nanofins originated from the edges, headed toward the center and finally terminated with a vertical NW. From the distribution of the nanofin structures, one can easily assume that they may reflect the moving trace of the catalyst clusters following the surface gradient. The epitaxial relationship between the NWs and the substrate was clearly revealed by a top view SEM image shown in Figure 3b, where all the NWs exhibited a hexagonal cross section. All of their six side surfaces were either parallel to or 60° from each other indicating the homoepitaxial growth of NWs on the thin film. However, such a relationship could not be observed from their attached nanofins. As shown in Figure 3c, all the tails aligned toward the center from random directions. Such randomness was demonstrated by the statistical result shown in Figure 3d. By defining a line that was parallel to one group of ZnO NW's side surfaces as the 0° line (as shown in Figure 3c), the angle between other nanofins and the 0° line was measured on >100 nanofin structures. The angle distribution shown in Figure 3d clearly shows that the orientation of the nanofins was completely random and nearly covered all possible angles without the preference of 60° intervals. This reveals that the nanofins might not be epitaxially initiated from the ZnO film or from the ZnO NW's side surfaces; instead, they most likely originated from the thermal drifting trace of the Zn clusters. Therefore, observing the distribution of the nanofins could reveal the dynamic process of the Zn cluster's moving behavior before it formed a NW.

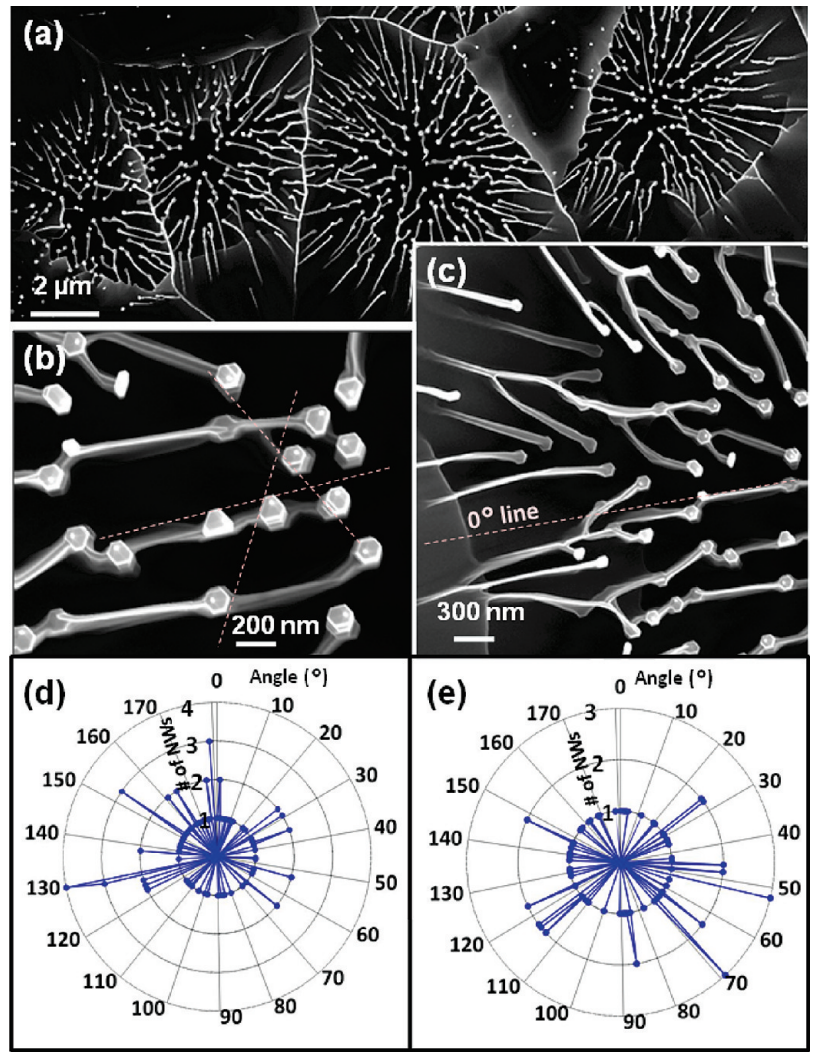

Figure 3. Angular dependence analysis of the drifting paths: (a) top view SEM image showing the overall drifting path distribution among the surface concaves; (b) top view SEM image of the NWs grown at the center of a concave. The three dashed lines (60° from each other) are guides to the eye; (c) top view SEM image of the nanofin structures on inclined concave surface. The 0° line was arbitrarily chosen along one side surface of a ZnO NW as a reference for determining the angular dependence; (d) statistical results of the angle distribution of the nanofins in the surface concaves; (e) statistical results of the angle distribution of the nanowalls grown on a flat surface (its structure is shown in Figure 4b).

In addition to the inclined crystal surface, the drifting behavior was also observed on flat crystal surfaces. By reducing the vapor concentration in the deposition chamber, the epitaxial ZnO layer growth was eliminated; while a small number of Zn clusters can still be precipitated from the vapor phase serving as catalysts. The drifting of Zn clusters was evidenced by small NWs winding around the GaN substrate (Figure 4a). Similarly, the moving of Zn clusters does not show any relationship to the (0001) surface of GaN, indicating such drifting was completely a Brownian motion. The drifting of Zn clusters was ceased by lowering the deposition temperature. Additional ZnO could still be deposited on the small cluster forming a relatively big tip (pointed by the arrows in Figure 4a) or even a small vertical NW if vapor source was sufficient.

This phenomenon could be used to explain the formation of ZnO nanowall network structures. Such a structure has been discovered by several research groups and the growth mechanisms were proposed to be epitaxial branching growth from the side walls or the root of ZnO NWs.[34,35,39,40] However, those proposed mechanisms could not explain the randomly orientated nanowalls, which typically did not exhibit any matching to the lattice orientation of either ZnO NWs or the substrate (Figure 4b). With the discovery of the thermally driven Brownian motion of Zn clusters, the formation of ZnO nanowall networks can now be fully understood. By adjusting the vapor concentration to a level that was favorable for rapid surface nucleation but still not high enough for epitaxial layer growth, the nanowall structure was formed (Figure 4b). All the walls

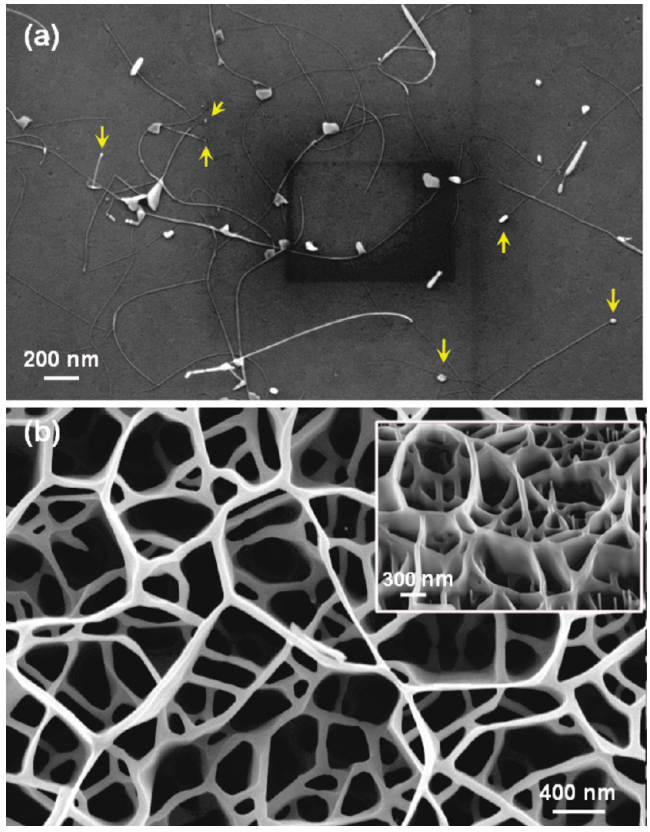

Figure 4. Zn cluster drifting phenomenon on a flat surface: (a) the random drifting traces visualized by the deposition of ZnO along the paths. The arrows are pointing at the heads of the drifting traces; (b) nanowall network structure formed by enabling a rapid surface nucleation to substantially increase the amount of Zn clusters. Inset is the side view of the nanowall network structure.

were perpendicular to the substrate (inset of Figure 4b) but their horizontal orientations were completely random. The orientation angle distribution was measured on ~80 nanowalls and the 0° line was arbitrarily chosen along one nanowall. As shown in Figure 3e, the orientation was unpreferentially distributed among all angles from 0−180° indicating that the substrate lattice had no influence on the nanowalls' horizontal orientation. It was the random thermal drifting of a large amount of Zn clusters that defined the distribution of the nanowall structure.

General Mechanisms of the Zn Cluster Drifting Phenomenon and the Resulted Nanostructures. By fully analyzing the growth phenomena induced by Zn cluster thermal drifting, one general mechanism could be concluded. At a relatively high temperature (~875 °C), the Zn clusters that were precipitated on the substrate through heterogeneous nucleation could drift and leave an active trace that was more favorable for further deposition through a vapor-solid process. The drifting resulted morphology will be discussed in two circumstances—on inclined surface and on flat surface.

On an inclined crystal surface, the Zn clusters intended to flow "down" along the surface driven by thermal vibration. However, we believe this tendency was more likely induced by the stepped-crystal surface, where the lattice step ledges below the Zn cluster were more energetic favorable places for Zn atoms to move onto (Figure 5a); while the crystal surface behind the cluster could be quickly flattened out by forming ZnO along the steps (Figure 5b). It should be noticed that at such a small scale, gravity typically has negligible effects on driving the movement of the clusters. This has been verified by depositing ZnO crystals at the same experimental condition on a vertically placed flat GaN substrate, where no downward moving traces of the deposited ZnO nanostructures were discovered.

Once the deposition temperature was reduced below ~700 °C so that the thermal energy became insufficient to drive the drifting of Zn cluster, or the Zn cluster reached the bottom flat area, where the limited space restricted its further movement, the Zn cluster would stay fixed and start to catalyze the growth of a NW. The growth of the NW created a new corner edge between the NW and the film formed along the moving trace. This corner was a thermodynamically favorable site for Zn atoms to diffuse to and to be adsorbed forming ZnO (Figure 5c). The ledges created along the moving trace were also thermodynamically favorable sites for additional ZnO deposition from vapor phase until they were flattened out. As a result, the nanofin film typically exhibited a relatively flat top surface with a slightly higher region near the NW (Figure 5d) due to the diffusion of Zn atoms from the NW.

When no lattice steps or other dislocations were present on the surface, the drifting of Zn clusters became completely random. At a relatively low Zn vapor supersaturation condition, low density nucleation occurred, where the nuclei were at least a few hundred nanometers away from each other. The growth mechanism under this situation is schematically shown in Figure 6a. The Brownian motion of the Zn cluster also left a visible trace by forming a horizontal ZnO NW. However, this trace could rarely grow into a vertical film as on the inclined surfaces, simply due to the absence of the stepped ledges serving as deposition sites. The drifting of Zn clusters could be stopped by merging with another moving trace, sticking on a substrate defect, or reducing the local temperature. With sufficient vapor supply after the clusters stopped moving, vertically aligned NWs grew out of the Zn clusters through a self-catalyzed VS process, as shown in Figure 6b, where the NWs grown at the end of the moving traces are indicated by arrows.

High density heterogeneous nucleation could occur at a slightly higher Zn vapor supersaturation and the corresponding growth mechanism is schematically shown in Figure 6c. Similarly, the Zn clusters would also move randomly at the beginning. However, because of the high density of the clusters, they would quickly collide with each other and cease their movements leaving a network-shaped trace of movement. In addition, those clusters would initiate vertical growth of ZnO NWs, which cre-

ated thermodynamic favorable corner edges between their side surfaces and the horizontal moving traces for ZnO deposition. Because of the higher vapor concentration and the small distance between ZnO NWs, the space between NWs could be quickly filled by a thin wall of ZnO crystal. Therefore, led by the growth of NWs, a continuous nanowall network could be formed. Since the nanowalls were originated from the Brownian motion traces of Zn clusters, their distribution did not follow the substrate lattice, although the entire film could be considered as a c-plane orientated epitaxial film.[40]

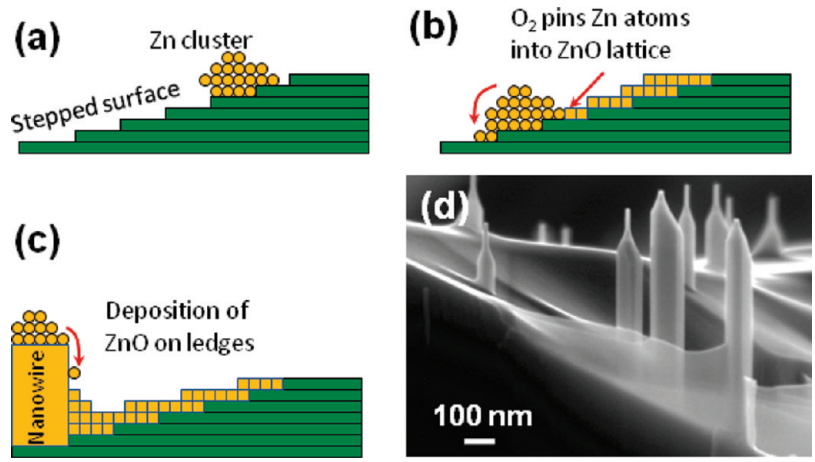

Figure 5. (a-c) Schematic mechanism of the Zn cluster drifting phenomenon on an inclined surface and the formation of NW-nanofin structure. (d) A cross-section image showing the height variance of the nanofin structure.

Application of the Drifting Phenomenon for Morphology Control. The discovery of catalyst drifting phenomenon would bring a new pathway for controlling the nanostructure morphology. The vertically grown thin film structure has been suggested as one promising model of a next generation high-density integrated circuit system, such as the Si-fin FETs.[41,42] To demonstrate a possible way to achieve control growth of the vertical ZnO nanofins, a line pattern of Au catalyst film coated substrate was created to confine the distribution of inclined base surfaces on GaN substrate. This is because high density NWs were typically formed with the existence of Au catalysts, while ZnO epitaxial layers were preferentially grown on the non-Au covered region. In the experiments, two types of patterns were applied for the growth control.

One type of pattern was a thin line (~5 μm wide) of exposed substrate sandwiched between two wide stripes of Au catalyst film. Under this situation, the growth of ZnO epitaxial layer was limited by the gold catalysts, which catalyzed the growth of NW forests. Therefore, the center of the exposed area exhibited the fastest growth rate thus formed a "hill" shaped ZnO epitaxial base layer, as shown in the inset of Figure 7a. Most Zn clusters were nucleated along the central line at the summit of the "hill", where the heterogenerous nucleation energy was minimized. Following the inclined base surface, Zn clusters drifted to the bottom of the "hill" and initiated the formation of ZnO nanofins that were approximately parallel to each other, as shown in Figure 7a. Because of the existence of a central wall, which possibly resulted from the dense nucleation sites along the summit, the vertical nanofins exhibited a more uniform height from their origin positions to their NW terminations (Figure 7b).

Another pattern was a thin line (~2 μm wide) of Au covered region sandwiched between two wide stripes of exposed substrate. Under this situation, a "valley" was formed between two inclined ZnO epitaxial base layers and high density ZnO NWs were grown along the "valley", as shown in the inset of Figure 7d. Similarly, ZnO vertical nanofins formed along the inclined base surfaces heading toward the center of "valley" (Figure 7d). The parallel aligned ZnO nanofin structures exhibit obvious morphological advantages over Si finFET fabricated *via* lithography processes. As shown in Figure 7c, the nanofin structure can be grown with ~20 nm in

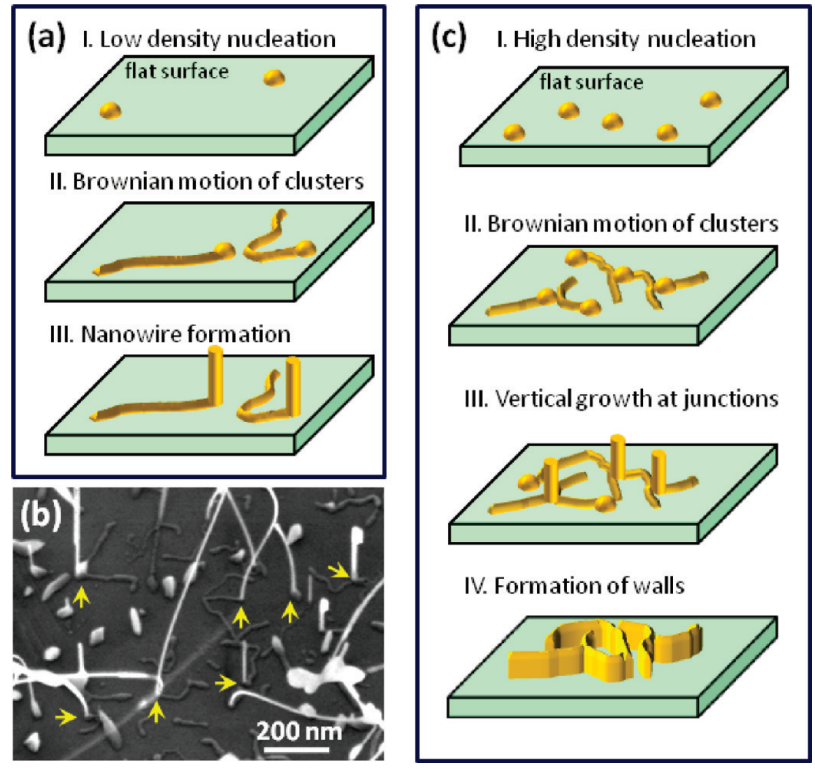

Figure 6. Mechanisms of the Zn cluster drifting on a flat surface. (a) The situation when the density of Zn cluster is low, where winding NWs on the surface were typically observed. (b) SEM image showing a vertical NW could also be grown after the cluster stopped moving, where the arrows pointing the NWs grown from the end of the surface drifting traces. (c) The situation when the density of Zn cluster is high, where a nanowall network structure can always be formed.

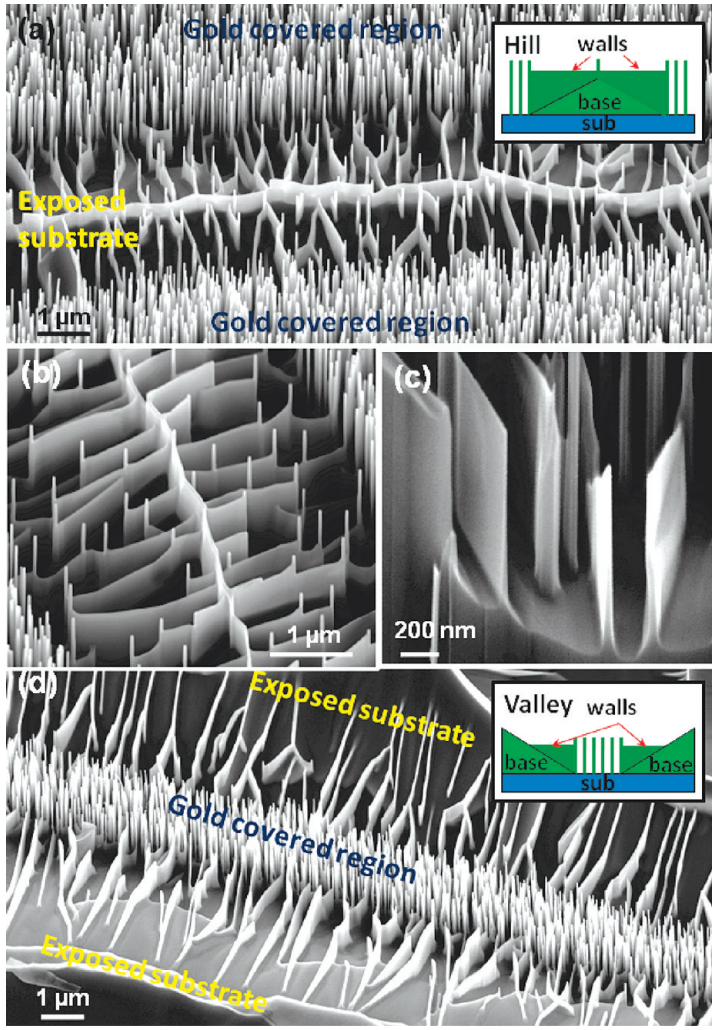

Figure 7. Formation of parallel aligned ZnO nanofin arrays by controlling the surface inclination: (a) ZnO nanofin arrays grown on a "hill" base formed between two wide stripes of nanowire forests. Inset shows a schematic illustration of such a configuration; (b) an approximately parallel aligned ZnO nanofin array showing a more uniform height distribution due to the formation of a center wall; (c) the cross-section of ZnO nanofins, which are only ~20 to 30 nm thick and ~1 μm tall (the one in the middle is terminated with a nanowire); (d) ZnO nanofin arrays grown in a "valley" base. Inset shows a schematic illustration of the "valley" configuration.

thickness and close to one micrometer in height. The as-synthesized side surfaces of the nanofins are very flat and smooth. Such a thin and vertical single-crystalline semiconductor film is greatly desired for constructing finFETs that can offer high current in a small footprint area and can effectively suppress the short channel effect.[41] Therefore, the self-assembled nanofin arrays would possibly serve as a promising novel 3D nanoconfiguration for finFET-based high performance nanoelectronic device development.

It should be noted that the onset temperature for catalyst drifting was found out to be ~700 °C in our system. Below this temperature, only perfectly aligned ZnO NWs were received without any side branches or nanowall networks. Although this catalyst drifting phenomenon was observed on Zn clusters in a ZnO deposition system, we believe this could be a general phenomenon that applies to most metal catalysts. Depending on the melting temperature, surface chemistry, and the metal-substrate interaction, the temperature needed to initiate the drifting should be different for different metal catalysts and substrates. Meanwhile, the drifting temperature should be maintained sufficiently high to avoid large super cooling of the source vapor, since quick precipitation from vapor phase under large super cooling would pin the catalysts onto substrate.

CONCLUSIONS

This paper presents a discovery of a Zn cluster thermal drifting phenomenon during the vapor deposition process of ZnO nanostructures. The dynamic drifting path of Zn clusters could be observed from the resulting ZnO nanofins or NWs initiated from the moving trace. The drifting of Zn clusters can be directed by the lattice steps along an inclined crystal surface and form vertically aligned nanofins along the trace. On a flat substrate surface, the drifting of Zn clusters was completely random and was not confined by the substrate lattice. This phenomenon provides a sound explanation of the formation of randomly orientated ZnO nanowall networks. By intentionally controlling the surface inclination to create directed drifting of Zn clusters, a parallel aligned ZnO nanofin 3D nanoarchitecture was realized. This nanofin array would possibly provide a novel configuration for designing high performance integrated nanodevices. The drifting of Zn clusters could be a general phenomenon for most metal catalysts and would provide a new insight into nanofabrication and nanodevice development.

METHODS

A horizontal tube furnace system was used to perform the vapor deposition of ZnO nanostructures. A small quartz tube 25 cm in length and 1.6 cm in inner diameter was used to support the precursor and substrate and increase the vapor concentration. In a typical process, ZnO powder (0.3 g) and graphite powder (0.3 g) were mixed and ground together and placed in a quartz boat positioned 5 cm from one end in the quartz tube. A 500-nm-thick GaN epilayer covered sapphire substrate was used for ZnO nanostructure deposition. Four pieces of the substrate

were placed inside the quartz tube, where the first substrate was 8 cm from the source boat, and the remainder were farther from the source and 3 cm from each other. This small quartz tube was then placed into a large alumina tube in the tube furnace with the source boat aligned at the center of the tube furnace and the substrates located on the downstream side of the carrier gas. The carrier gas used throughout the experiments was 1% oxygen balanced by high purity argon. First, the furnace was quickly increased to 925 °C at a ramp rate of 50 °C/min. When the temperature reached 400 °C, the carrier gas was introduced into the deposition system with a flow rate of 50 sccm and the system pressure was brought to 20 Torr. Then the furnace temperature was held at 925 °C for 30 min for ZnO nanostructure deposition. At this temperature, according to the temperature profile of this furnace, the local substrate temperatures were 900, 875, 700, 550 °C, respectively. Finally, the furnace was turned off and the system was allowed to cool down naturally without changing the system pressure and carrier gas flow. The morphology and structure of the as-synthesized ZnO nanostructures were characterized using SEM (LEO 1530) and TEM (Philips CM 200).

Acknowledgment. The authors are grateful for financial support from U.W. Graduate School.

REFERENCES AND NOTES

1. Lijima, S. Helical Microtubules of Graphitic Carbon. *Nature* **1991**, *354*, 56–58.
2. Xia, Y.; Yang, P.; Sun, Y.; Wu, Y.; Mayers, B.; Gates, B.; Yin, Y.; Kim, F.; Yan, H. One-Dimensional Nanostructures: Synthesis, Characterization, and Applications. *Adv. Mater.* **2003**, *15*, 353–389.
3. Thelander, C.; Agarwal, P.; Brongersma, S.; Eymery, J.; Feiner, L. F.; Forchel, A.; Scheffler, M.; Riess, W.; Ohlsson, B. J.; Gösele, U.; Samuelson, L. Nanowire-Based One-Dimensional Electronics. *Mater. Today* **2006**, *9*, 28–35.
4. Lu, W.; Lieber, C. M. Semiconductor Nanowires. *J. Phys. D: Appl. Phys.* **2006**, *39*, R387−R406.
5. Huang, Y.; Duan, X.; Cui, Y.; Lauhon, L.; Kim, K.; Lieber, C. M. Logic Gates and Computation from Assembled Nanowire Building Blocks. *Science* **2001**, *294*, 1313–1317.
6. Ahn, J. H.; Kim, H. -S.; Lee, K. J.; Jeon, S.; Kang, S. J.; Sun, Y.; Nuzzo, R. G.; Rogers, J. A. Heterogeneous Three-Dimensional Electronics by Use of Printed Semiconductor Nanomaterials. *Science* **2006**, *314*, 1754–1757.
7. Law, M.; Sirbuly, D.; Johnson, J.; Goldberger, J.; Saykally, R.; Yang, P. Nanoribbon Waveguides for Subwavelength Photonics Integration. *Science* **2004**, *305*, 1269–1273.
8. Barrelet, C. J.; Greytak, A. B.; Lieber, C. M. Nanowire Photonic Circuit Elements. *Nano Lett.* **2004**, *4*, 1981–1985.
9. Kim, H. M.; Kang, T. W.; Chung, K. S. Nanoscale Ultraviolet-Light-Emitting Diodes Using Wide-Bandgap Gallium Nitride Nanorods. *Adv. Mater.* **2003**, *15*, 567–569.
10. Huynh, W. U.; Dittmer, J. J.; Alivisatos, A. P. Hybrid Nanorod−Polymer Solar Cells. *Science* **2002**, *295*, 2425–2427.
11. Johnson, J. C.; Choi, H. J.; Knutsen, K. P.; Schaller, R. D.; Yang, P. D.; Saykally, R. J. Single Gallium Nitride Nanowire Lasers. *Nat. Mater.* **2002**, *1*, 106–110.
12. Wong, W. W.; Sheehan, P. E.; Lieber, C. M. Nanobeam Mechanics: Elasticity, Strength, and Toughness of Nanorods and Nanotubes. *Science* **1997**, *277*, 1971–1975.
13. Bai, X. D.; Gao, P. X.; Wang, Z. L.; Wang, E. G. Dual-Mode Mechanical Resonance of Individual ZnO Nanobelts. *Appl. Phys. Lett.* **2003**, *82*, 4806–4808.
14. Lavrik, N. V.; Datskos, P. G. Femtogram Mass Detection Using Photothermally Actuated Nanomechanical Resonators. *Appl. Phys. Lett.* **2003**, *82*, 2697–2699.
15. Snow, E. S.; Perkins, F. K.; Houser, E. J.; Badescu, S. C.; Reinecke, T. L. Chemical Detection with a Single-Walled Carbon Nanotube Capacitor. *Science* **2005**, *307*, 1942–1945.
16. Kong, J.; Franklin, N. R.; Zhou, C. W.; Chapline, M. G.; Peng, S.; Cho, K. J.; Dai, H. J. Nanotube Molecular Wires as Chemical Sensors. *Science* **2000**, *287*, 622–625.
17. Patolsky, F.; Timko, B. P.; Yu, G.; Fang, Y.; Greytak, A. B.; Zheng, G.; Lieber, C. M. Detection, Stimulation, and Inhibition of Neuronal Signals with High-Density Nanowire Transistor Arrays. *Science* **2006**, *313*, 1100–1104.
18. Huang, M. H.; Wu, Y.; Feick, H.; Tran, N.; Weber, E.; Yang, P. Catalytic Growth of Zinc Oxide Nanowires by Vapor Transport. *Adv. Mater.* **2001**, *13*, 113–116.
19. Pan, Z. W.; Dai, Z. R.; Wang, Z. L. Nanobelts of Semiconducting Oxides. *Science* **2001**, *291*, 1947–1949.
20. Huang, M. H.; Mao, S.; Feick, H.; Yan, H.; Wu, Y.; Kind, H.; Weber, E.; Russo, R.; Yang, P. Room-Temperature Ultraviolet Nanowire Nanolasers. *Science* **2001**, *292*, 1897–1899.
21. Look, D. C.; Claflin, B. *p*-Type Doping and Devices Based on ZnO. *Phys. Stat. Sol., b* **2004**, *241*, 624–630.
22. Ozgur, U.; Alivov, Y. I.; Liu, C.; Teke, A.; Reshchikov, M. A.; Dogan, S.; Avrutin, V.; Cho, S.-J.; Morkoc, H. A Comprehensive Review of ZnO Materials and Devices. *J. Appl. Phys.* **2005**, *98*, 041301(1)041301(103) .
23. Wang, X. D.; Song, J. H.; Wang, Z. L. Nanowire and Nanobelt Arrays of Zinc Oxide from Synthesis to Properties and to Novel Devices. *J. Mater. Chem.* **2007**, *17*, 711–720.
24. Wang, X. D.; Song, J. H.; Liu, J.; Wang, Z. L. Direct-Current Nanogenerator Driven by Ultrasonic Waves. *Science* **2007**, *316*, 102–105.
25. Wang, Z. L.; Wang, X. D.; Song, J. H.; Liu, J.; Gao, Y. F. Piezoelectric Nanogenerators for Self-Powered Nanodevices. *IEEE Perv. Comp.* **2008**, *7*, 49–55.
26. Wang, X. D.; Summers, C. J.; Wang, Z. L. Large-Scale Hexagonal-Patterned Growth of Aligned ZnO Nanorods for Nano-optoelectronics and Nanosensor Arrays. *Nano Lett.* **2004**, *4*, 423–426.
27. Gudiksen, M. S.; Wang, J.; Lieber, C. M. Synthetic Control of the Diameter and Length of Single Crystal Semiconductor Nanowires. *J. Phys. Chem. B* **2001**, *105*, 4062–4064.
28. Wu, Y.; Yang, P. Direct Observation of Vapor−Liquid−Solid Nanowire Growth. *J. Am. Chem. Soc.* **2001**, *123*, 3165–3166.
29. Wang, Z. L.; Kong, X. Y.; Zuo, J. M. Induced Growth of Asymmetric Nanocantilever Arrays on Polar Surfaces. *Phys. Rev. Lett.* **2003**, *91*, 185502(1)185502(4) .
30. Ross, F. M.; Tersoff, J.; Reuter, M. C. Sawtooth Faceting in Silicon Nanowires. *Phys. Rev. Lett.* **2005**, *95*, 146104(1)146104(4) .
31. Hannon, J. B.; Kodambaka, S.; Ross, F. M.; Tromp, R. M. The Influence of the Surface Migration of Gold on the Growth of Silicon Nanowires. *Nature* **2006**, *440*, 69–71.
32. Tersoff, J.; Tromp, R. M. Shape Transition in Growth of Strained Islands: Spontaneous Formation of Quantum Wires. *Phys. Rev. Lett.* **1993**, *70*, 2782–2785.
33. Nikoobakht, B.; Michaels, C. A.; Stranick, S. J.; Vaudin, M. D. Horizontal Growth and *in Situ* Assembly of Oriented Zinc Oxide Nanowires. *Appl. Phys. Lett.* **2004**, *85*, 3244–3246.
34. Grabowska, J.; Meaney, A.; Nanda, K. K.; Mosnier, J.-P.; Henry, M. O.; Duclère, J.-R.; McGlynn, E. Surface Excitonic Emission and Quenching Effects in ZnO Nanowire/Nanowall Systems: Limiting Effects on Device Potential. *Phys. Rev. B* **2005**, *71*, 115439(1)115439(7) .
35. Ng, H. T.; Li, J.; Smith, M. K.; Nguyen, P.; Cassell, A.; Han, J.; Meyyappan, M. Growth of Epitaxial Nanowires at the Junctions of Nanowalls. *Science* **2003**, *300*, 1249.
36. Wang, X. D.; Song, J.; Li, P.; Ryou, J. H.; Dupuis, R. D.; Summers, C. J.; Wang, Z. L. Growth of Uniformly Aligned ZnO Nanowire Heterojunction Arrays on GaN, AlN, and $Al_{0.5}Ga_{0.5}N$ Substrates. *J. Am. Chem. Soc.* **2005**, *127*, 7920–7923.
37. Gao, H.; Nix, W. D. Surface Roughening of Heteroepitaxial Thin Films. *Annu. Rev. Mater. Sci.* **1999**, *29*, 173–209.
38. Yang, R. S.; Wang, Z. L. Interpenetrative and Transverse Growth Process of Self-Catalyzed ZnO Nanorods. *Solid State Commun.* **2005**, *134*, 741–745.

39. Lao, J. Y.; Huang, J. Y.; Wang, D. Z.; Ren, Z. F.; Steeves, D.; Kimball, B.; Porter, W. ZnO Nanowalls. *Appl. Phys. A: Mater. Sci. Process.* **2004**, *78*, 539–542.
40. Wang, X. D.; Ding, Y.; Li, Z.; Song, J.; Wang, Z. L. Single-Crystal Mesoporous ZnO Thin Films Composed of Nanowalls. *J. Phys. Chem. C* **2009**, *113*, 1791–1794.
41. Colinge, J. P. FinFETs and Other Multi-Gate Transistors; Springer: New York , 2007; p 1340..
42. Hisamoto, D.; Lee, W. C.; Kedzierski, J.; Takeuchi, H.; Asano, K.; Kuo, C.; Anderson, E.; King, T. J.; Bokor, J.; Hu, C. FinFET-A Self-Aligned Double-Gate MOSFET Scalable to 20 nm. *IEEE Trans. Electron Devices* **2000**, *47*, 2320–2325.